Human Pathology (2019) **84**, 262–269

ELSEVIER

Human PATHOLOGY

www.elsevier.com/locate/humpath

Original contribution

Detection of H3K27M mutation in cases of brain stem subependymoma☆

Kun Yao MD[a,1], Zejun Duan MS[a,1], Yin Wang MD[b], Mingshan Zhang MD[c], Tao Fan MD[c], Bin Wu BS[c], Xueling Qi BS[a,*]

[a]*Department of Pathology, San Bo Brain Hospital, Capital Medical University, Haidian District, Beijing, China*
[b]*Department of Pathology, Huashan Hospital, Shanghai Medical College, Fudan University, Shanghai 200040, China*
[c]*Department of Neurosurgery, San Bo Brain Hospital, Capital Medical University, Haidian District, Beijing, China*

Received 5 August 2018; revised 2 October 2018; accepted 11 October 2018

Keywords:
H3K27M mutation;
Subependymoma;
Brain stem neoplasm;
Sanger sequencing

Summary Subependymomas are rare, slow-growing, grade I glial tumors of the central nervous system. Recently, diffuse midline gliomas with mutations in the H3.1 or H3.3 genes at the position of amino acid 27, resulting in the replacement of lysine by methionine (K27M), were defined as the new grade IV entity. As H3K27M mutations have been reported in midline gliomas, gangliogliomas, and pilocytic astrocytomas, whether they occur in midline subependymomas has been unclear. We determined whether any such mutations can be found in them and analyzed the prognostic relevance of any such mutations in subependymomas. Four subependymomas, all in the brain stem, harbored H3K27M mutations. No such mutation was found in any of the subependymomas from other locations. The mutations were identified by immunohistochemical stains and confirmed with Sanger sequencing. The median follow-up of the patients with the mutations in their tumors was 3.2 years, and 3 are still alive, having received no adjuvant therapy. We demonstrate that H3K27M mutation can occur in brainstem subependymomas; despite the presence of H3K27M mutation, these cases should not be diagnosed or treated as grade IV tumors because they showed a better outcome than the outcome of diffuse midline H3K27M mutant glioma. Our conclusion is not only that brainstem subependymomas can have H3K27M mutations but that they do not carry the rapidly lethal prognosis with which these mutations are usually associated because of their discovery in diffuse intrinsic pontine gliomas.

1. Introduction

Subependymomas are rare primary central nervous system (CNS) tumors that occur mostly in middle-aged and elderly men [1,2]. They account for 0.07%-0.51% of brain tumors and are considered grade I benign tumors in the 2016 revision of the WHO classification of CNS tumors [3]. Long-term survival is generally excellent even if the entire subependymoma cannot be removed [4,5]. The most common locations are in

☆ Disclosures: none.

* Corresponding author.
E-mail addresses: yaokun2007@163.com (K. Yao), night0329@gmail.com (Z. Duan), Wangyin8wangyin@163.com (Y. Wang), Zhangms7606@sina.com (M. Zhang), fantao971@163.com (T. Fan), wubin0324@sina.com (B. Wu), xszqxl169@163.com (X. Qi).
[1] Kun Yao and Zejun Duan are co-first authors.

https://doi.org/10.1016/j.humpath.2018.10.011
0046-8177/

Table 1 Clinical characteristics of the subependymomas and grade II or grade III anaplastic ependymomas examined in this study

Diagnosis	n	Age, median (range)	Sex	Location (no. of cases)	H3K27M genotype
Subependymoma	24	41.5 (13-61)	18 M; 6 F	Brain stem (4) Temporal lobe (3) Spinal cord (5) Lateral ventricle (12)	H3K27M mutation Wild type (20)
Grade II ependymoma	18	40.29 (12-61)	15 M; 3 F	Brain stem (1) Fourth ventricle (5) Frontal lobe (2) Spinal cord (10)	Wild type (18)
Grade III ependymoma	13	12.1 (2-31)	8 M; 5 F	Brain stem (1) Fourth ventricle (5) Frontal lobe (2) Temporal lobe (1) Cerebellum (2) Spinal cord (2)	Wild type (13)

Abbreviations: F, female; M, male.

one of the lateral ventricles [1], but they also occur in the fourth ventricle, within the brain parenchyma, and in the spinal cord [4-7]. Rare subependymomas are found in the brain stem [8]. Subependymoma in brain stem exhibited a poorer prognosis [8]. However, it remains unclear whether this poor prognosis is due to their location-related incomplete resection or due to their molecular features.

H3K27M glioblastomas are located in the midline and have been shown to have worse prognosis than other GBM subgroups, with a median survival of 6 months [3,9,10]. Recent case reports have described the H3K27M mutation in certain midline low-grade tumors, such as pilocytic astrocytomas and other glioneuronal tumors [11-14], which suggest that H3K27M mutations may be present in a spectrum of low-grade glial tumors and mixed glioneuronal tumors, located in midline areas, without necessarily signifying a poor prognosis [11,13]. The frequency of H3K27M mutation in subependymoma, especially in the brain stem subependymoma, is unknown. In this study, we searched for H3K27M mutations in a series of 24 diagnosed subependymomas using a combination of immunohistochemistry (IHC) and Sanger sequencing.

2. Materials and methods

2.1. Tumor samples

We studied 24 cases of grade I subependymoma, as defined by the WHO classification criteria, between March 2008 and November 2017. We searched their files for cases of subependymoma and retrieved slides and blocks for 24 cases. All cases were independently reviewed by 2 pathologists of SanBo Brain Hospital. Disagreements in evaluation were resolved by review and discussion at a multiheaded microscope. The slides verified the diagnoses as subependymoma by the WHO 2016 criteria. All the selected cases presented typical features of subependymomas, which are the loose clusters of small bland round nuclei in a dense fibrillary matrix of glial cell processes with frequent occurrence of small cysts and occasionally exhibiting pseudorosettes. Sections for IHC and genetic analyses were prepared from formalin-fixed, paraffin-embedded tissue specimens.

A range of other brain tumors was also investigated and included the ependymomas (WHO grade II) (n = 18) and the anaplastic ependymomas (WHO grade III) (n = 13). The clinical characteristics of the patients with subependymomas are summarized in Table 1.

2.2. IHC analyses of H3F3A, HIST1H3B, and HIST1H3C

Representative formalin-fixed sections were deparaffinized and stained with hematoxylin and eosin (H&E) and IHC according to immunohistochemical reagent instructions. In brief, 4-μm sections were deparaffinized. The sections were then treated with 3% H_2O_2 for 5 minutes at room temperature to block endogenous peroxidase activity. For antigen retrieval, slides were pretreated by steaming in sodium citrate buffer for 15 minutes at 100°C. Then, the slides were blocked with 5% fetal bovine serum at room temperature for 15 minutes and incubated with primary antibodies against GFAP (Dako,1:150), Olig-2 (Dako,1:100), EMA (Leica,1:100), Ki-67 (Dako,1:100), IDH1-R132H (Dianova, Germany,1:60), ATRX (Abcam, 1:800), TP53 (Santa Cruz Biotechnology, 1:200), H3K27M (EMD Millipore, 1:3000), and H3K27me3 (Cell Signaling Technology, 1:300) at 4°C overnight. After being washed with phosphate-buffered saline, the sections were covered by anti-mouse/rabbit polymer HRP-label for 30 minutes. Then, DAB was applied for color development at room temperature for 5 minutes, and sections were subsequently counterstained with hematoxylin. Each slide was individually

Table 2 Histological characteristics of the 24 subependymomas examined in this study

Markers	Marker-expressing cases (%)
GFAP	
+	24 (100%)
−	0
Olig-2	
+	0
−	24 (100%)
H3K27M	
+	4 (16.7%)
−	20 (83.3%)
H3k27me3	
+	20 (83.3%)
−	4 (16.7%)
EMA	
+	11 (45.8%)
−	13 (54.2%)
ATRX	
+	24 (100%)
−	0
IDH1R132H	
+	0
−	24 (100%)
TP53	
+	0
−	24 (100%)

NOTE. The expression levels were based on the percentages of the immunopositive cells (negative, <10% of tumor cells; positive, ≥10% of tumor cells).

reviewed and scored by 2 experienced neuropathologists. In case of disagreement, the slide was reexamined, and a consensus was reached by the observers. Ki-67 was scored as the percentage of nuclei-stained cells out of all tumor cells in ×400 high-power field; about 1000 tumor cells were counted overall for an entire slide. Adequate positive and negative controls were stained in parallel. Clinical features were obtained by reviewing the respective clinical records or by contacting the referring physicians. The study was approved by the Institutional Review Board of the SanBo Brain Hospital.

2.3. Mutation analyses of *H3F3A, HIST1H3B*, and *HIST1H3C*

2.3.1. DNA extraction

Areas of the specimens that were enriched in tumor cells were marked on the H&E-stained sections. Tissue was scraped from this preselected area and transferred to an Eppendorf tube for DNA isolation using the QIAamp DNA Mini kit (Qiagen GmbH, Germany) in accordance with the manufacturer's protocol. The quality and concentration of DNA samples were examined using a spectrophotometer (Biophotometer Eppendorf, Germany).

2.3.2. Sanger sequencing

Histone *H3F3A*, *HIST1H3B*, and *HIST1H3C* were analyzed by direct sequencing of polymerase chain reaction–

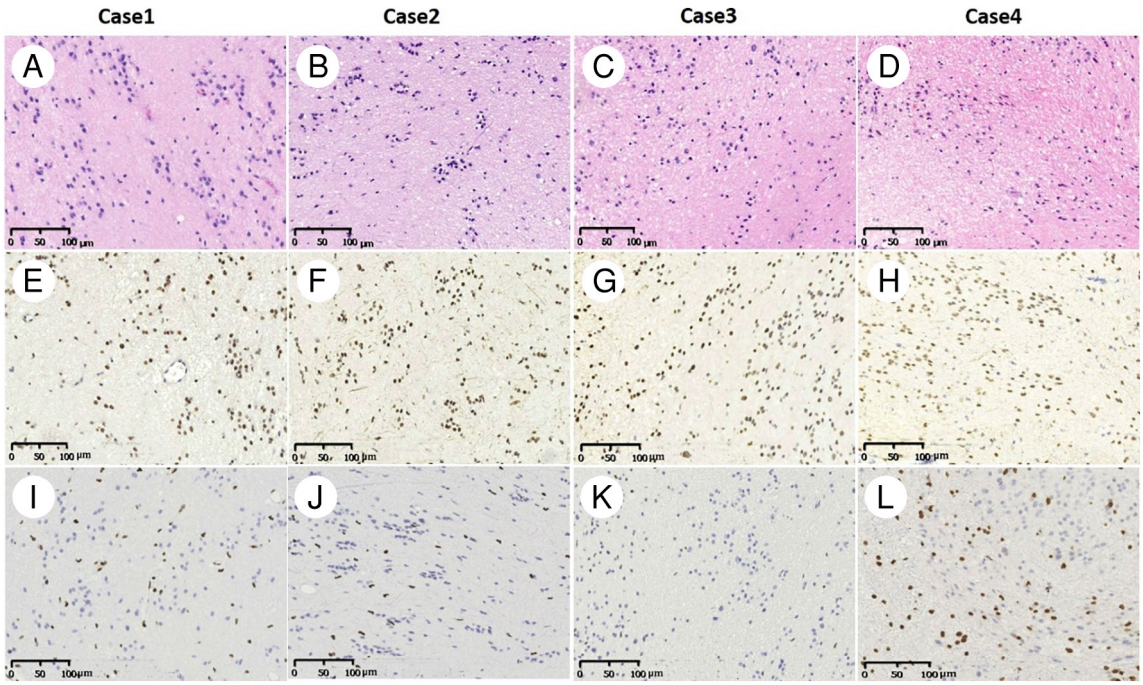

Fig. 1 Histological and immunohistochemical analyses of 4 cases of subependymoma in brain stem with the H3K27M mutations. A-D, H&E revealed the diagnosis of subependymomas. Tumors cells showed magnification 100. IHC staining of 4 cases of subependymomas in brain stem using anti-H3K27M (E-H) and anti-H3K27me3 (I-L) antibodies. E-H, H3K27M shows strong nuclear positivity in tumor cells but no staining in the nuclei of endothelial and smooth muscle cells in blood vessels. I-L, Accordingly, H3K27me3 staining on the same samples shows loss of the expression of this histone marker in H3K27M mutant tumors.

amplified products from tumor DNA using the primers previously described [15]. The amplified products were studied by direct sequencing after clean-up exonuclease ExoSAP-IT (Affymetrix, Santa Clara, CA) using the Big Dye Terminator Cycle Sequencing Kit and capillary electrophoresis on the automated sequencer ABI3730 (Applied Biosystems, Carlsbad, CA). Sense and antisense sequences were screened for exonic alterations using SeqScape v2.5software (Applied Biosystems) and compared with the National Center for Biotechnology Information reference sequences of *H3F3A*, *HIST1H3B*, and *HIST1H3C*.

2.3.3. *BRAF*V600E mutation analysis

DNA was quantified to a final concentration of 2 ng/μL. *BRAF*V600E mutations were analyzed with an amplification-refractory mutation system using AmoyDx BRAF V600E Mutation Detection Kit (Amoy Diagnostics) according to the manufacturer's instructions. The FAM fluorescence signal was used to evaluate the mutation status of the sample. When the sample FAM Ct value was ≥28, the sample was classified as negative or being below the detection limit of the kit. When the sample FAM Ct value was <28, the sample was classified as mutation positive.

2.3.4. Fluorescence in situ hybridization

Formalin-fixed, paraffin-embedded blocks were analyzed via fluorescence in situ hybridization (FISH) using the techniques previously described. Briefly, 5-μm–thick formalin-fixed, paraffin-embedded sections were incubated at 56°C for 2 hours, dewaxed, air dried, and

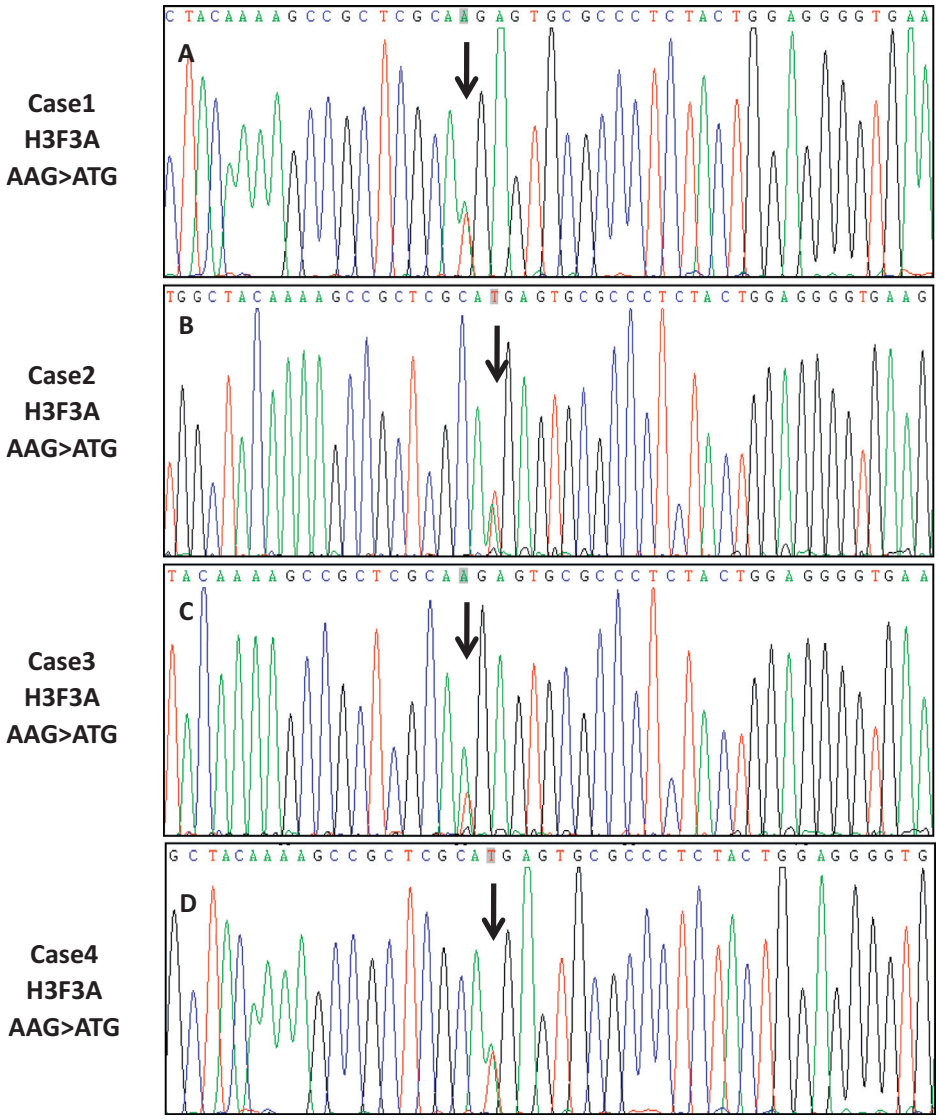

Fig. 2 A-D, Mutation analysis of H3F3A in cases of 1-4 showing G>T mutation. Sanger sequencing chromatograph of resulting polymerase chain reaction–amplified H3F3A confirmed c.83A>T transversion in DNA of cases of 1-4 tumor tissues (arrow).

dehydrated. Specimen were boiled in heat pretreatment solution for 40 minutes at 90°C, washed in 2× saline sodium citrate (SSC), digested with the enzyme reagent for 10 minutes at 37°C, washed in 2× SSC, dehydrated, and air dried. The KIAA1549 (green; Agilent Technologies)/BRAF (red; Agilent Technologies) probe mix was applied to the selected hybridization area for the fusion gene product of KIAA1549 and BRAF. Dual-color FISH was applied to the selected hybridization area using locus-specific identifier (LSI) 1p36/LSI 1q25 (Vysis/Abbott Molecular) and LSI 19q13/19p13 dual-color probe (Vysis/Abbott Molecular) for loss of 1p36/19q13. The selected hybridization area was covered with a coverslip and sealed with rubber cement. DNA co-denaturation was performed at 85°C for 5 minutes, and hybridization was allowed to occur at 38°C for 14-18 hours. Posthybridization washes were performed by incubating in 2× SSC at 37°C for 10 minutes and then 2× SSC/0.1% NP-40 at room temperature for 5 minutes, followed by dehydration. Finally, 4′,6-diamidino-2-phenylindole was applied, and the area was covered with a coverslip.

Tumors were scored as positive for the *BRAF-KIAA1549* fusion when >20% of the cells demonstrated yellow signals (indicating overlap of the green and red signals) in at least 100 nonoverlapping, intact nuclei. The total number of signals was counted, and a ratio of 1p:1q (or 19q:19p) of <0.75 was diagnosed as loss (losses of 1p36/19q13).

3. Results

3.1. Clinical characteristics

3.1.1. Subependymoma

The clinical characteristics of the cases with subependymoma studied here are summarized in Table 1. The study cohort was composed of 18 (75%) male and 6 (25%) female patients, with a median age at surgery of 45 years (range: 13-61 years). Twelve tumors were in a lateral ventricle, 5 in the spinal cord, 4 in the brain stem, and 3 in the temporal lobe.

3.1.2. Ependymomas (WHO grade II and WHO grade III)

The clinical characteristics of the 18 patients with grade II ependymoma and 13 patients with grade III anaplastic ependymoma are summarized in Table 1. The grade II ependymomas were from 15 male and 3 female patients, with a median age at surgery of 40.29 years (range: 12-61 years). Ten tumors were in the spinal cord, 5 in the fourth ventricle, 2 in the frontal lobe, and 1 in the brain stem.

The grade III anaplastic ependymomas were from 8 male and 5 female patients, with a median age at surgery of 12.1 years (range: 2-31 years). Five of these were in the fourth ventricle; 2 each were in the cerebellum, spinal cord, and frontal lobe; and 1 each was in temporal lobe and brain stem.

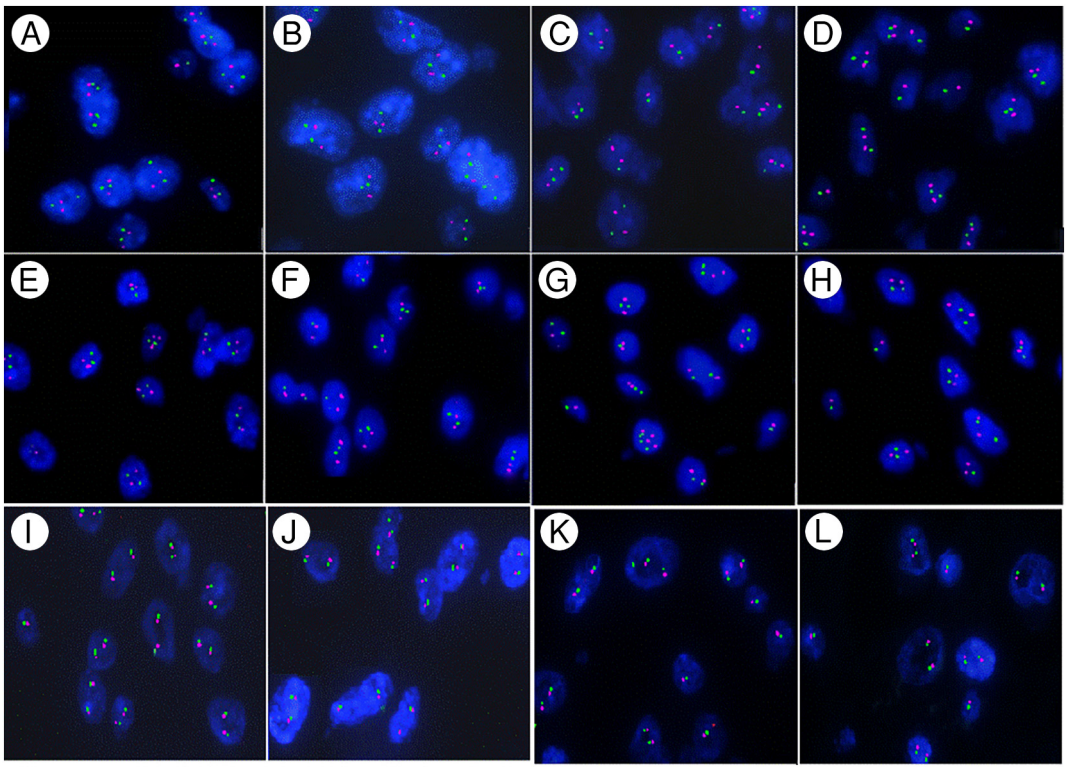

Fig. 3 FISH performed on the 4 cases for detecting the chromosome 1p36 and 19q13 and for the *BRAF-KIAA1549* fusion. Case 1 tumor cells showed no deletion of 1p36 (A) and 19q13 (B); case 2 tumor cells showed no deletion of 1p36 (C) and 19q13 (D); case 3 tumor cells showed no deletion of 1p36 (E) and 19q13 (F); case 4 tumor cells showed no deletion of 1p36 (G) and 19q13 (H). Case 1 (I), case 2 (J), case 3 (K), and case 4 (L) tumor cells showed no *BRAF-KIAA1549* fusion.

Table 3 Clinical features of the 4 cases of subependymoma with H3K27M mutations

	Sex	Years at diagnosis	Location	Gross total resection	Adjuvant treatment	Follow-up period	Follow-up	Status at follow-up
Case 1	M	24	Pons	No	No	5 y	Stability of the residual tumor	Alive
Case 2	M	43	Medulla oblongata	No	No	3.1 y	Tumor recurrence in situ	Dead
Case 3	M	13	Pons	No	No	3.3 y	Stability of the residual tumor	Alive
Case 4	M	20	Pons	No	No	0.25 y	Stability of the residual tumor	Alive

3.2. Pathological characteristics

The histological characteristics of the subependymoma in all 24 cases contained a coarse fibrillar matrix, with clusters of small uniform nuclei. Microcysts were common and were found in 18 (75%) tumors. None of the cases contained necrosis and microvascular proliferation. These tumors exhibited low-level mitotic activity, and the Ki-67 was less than 5% in any of tumors (Table 2). All of the tumors were immunopositive for GFAP. All had nuclear ATRX immunoreactivity (and so there was no ATRX mutation). No subependymoma was immunopositive for Olig2, TP53, or the protein product of the IDH1 R132H mutation. Eight had EMA immunoreactivity (Table 2).

H3K27M status was determined by IHC and Sanger sequencing. H3K27M immunoreactivity was only observed in the 4 subependymomas from the brain stem (Tables 1 and 2, and Fig. 1E-H). The histological evaluation showed typical morphology of subependymoma (Fig. 1A-D). All 4 of the H3K27M immunopositive tumors were confirmed to have the mutations by Sanger sequencing (*H3F3A* K27 M, AAG > ATG) (Fig. 2). No mutation in *HIST1H3B* or *HIST1H3C* gene was found. In the tumors with H3K27M mutations, there was loss of immunoreactivity for H3K27Me3 (Fig. 1I-L). FISH for 1p/19q co-deletion and *BRAF-KIAA1549* fusion and amplification-refractory mutation system methods for detecting *BRAF*V600E mutation were available for 4 brain cases. *BRAF*V600E mutation and *BRAF-KIAA1549* fusion (Fig. 3I-

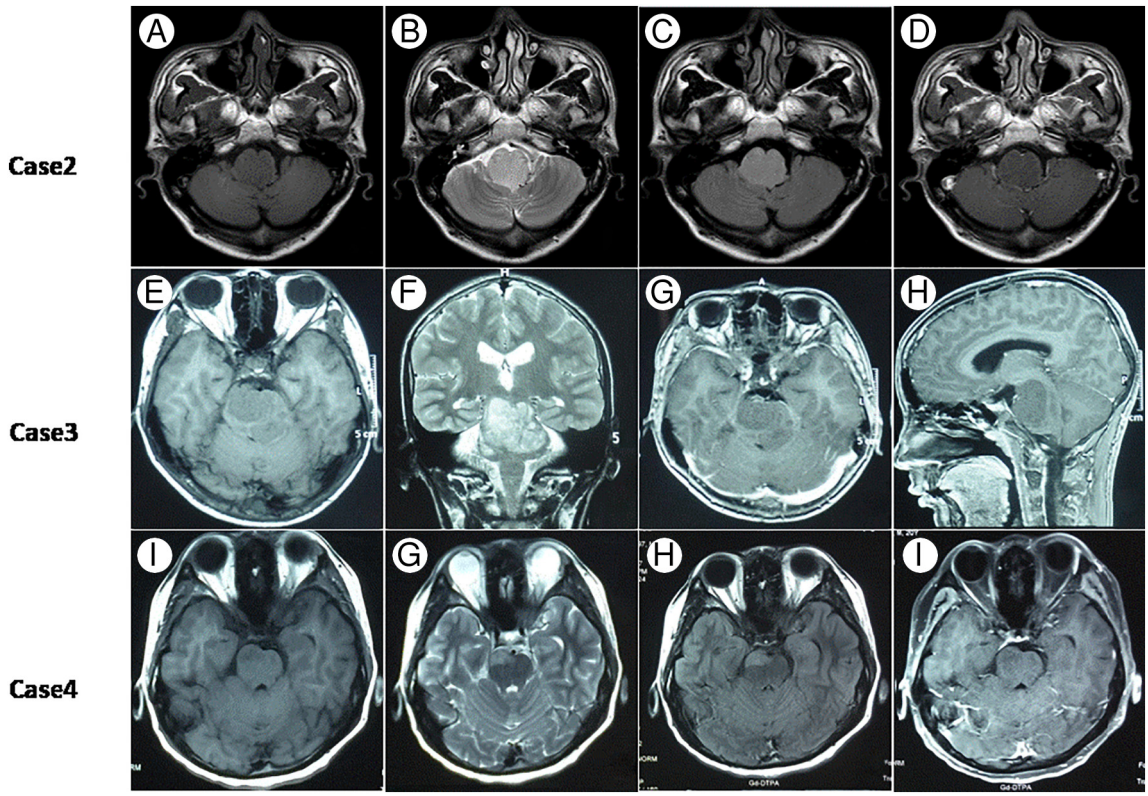

Fig. 4 The preoperative radiologic imaging of cases 2, 3, and 4. These tumors were all isointense to gray matter in T1-weighted MRIs (A, E, and I) and were slightly hyperintense compared to gray matter in T2-weighted (B, F, and G) and FLAIR sequences (C and H), but contrast-enhanced MRIs showed no enhancement (D, G, H, and I).

L) were not found in 4 patients. No 1p/19q co-deletion was detected in 4 cases (Fig. 3A-H).

H3K27M mutations were not found in any of the grade II or grade III ependymomas (Table 1). Tumors without H3K27M mutations all displayed H3K27me3.

3.2.1. Clinical features of the 4 H3K27M mutant brain stem subependymomas

The clinical and radiological characteristics of the 4 patients with H3K27M mutations are summarized in Table 3 and Fig. 3. These patients had a median age of 22 years (range: 13-43 years). All 4 patients were male. The tumors were located in the medulla oblongata and pons. The tumors in case 1, 3, and 4 were removed through right frontotemporal-subtemporal approach. The tumor in case 2 was removed through posterior median approach. No gross total resection was performed. The patients are still alive at 60, 39.6, and 3 months postsurgery, and 1 died at 37.2 months. The median overall survival, defined by the follow-up period, was 3.2 years (range: 0.25-5 years). None of the patients received post-surgical treatment (radiotherapy and chemotherapy).

These tumors were all isointense to gray matter in T1-weighted magnetic resonance images (MRIs) (Fig. 4A, E, and I) and were slightly hyperintense compared to gray matter in T2-weighted (Fig. 4B, F, and G) and FLAIR sequences (Fig. 4C and H), but contrast-enhanced MRIs showed no enhancement (Fig. 4D, G, H, and I).

4. Discussion

We have described 4 cases of brain stem subependymoma with H3K27M mutations, whereas 20 others from other CNS sites lacked such mutations. Ours is the first report of such mutations in subependymomas. All 4 of the tumors were histologically ordinary grade I examples without any features of high-grade gliomas, and 3 of the 4 patients are still alive without evidence of progressive disease despite having undergone only partial resections without any adjunctive therapy. This finding is in considerable contrast to the survival of diffuse midline gliomas with H3K27M mutations and is similar to the reported good survival of a child with a pilocytic astrocytoma with such a mutation [16] or the long survival reported for some patients with midline gangliogliomas or other glioneuronal tumors with such mutations [11,13].

The H3K27M mutation has been described in midline low-grade glial tumors and glial-neuronal tumors [11-14], even in 2 cases of posterior fossa ependymoma [17]. All together, these data suggest that H3K27M mutation is not specific to malignant grade IV glial tumor. In agreement with the evaluated H3K27M expression, we identified a global reduction in H3K27me3 in tumors with H3K27M mutation compared to tumors without H3K27M mutation, which is in line with previous reports [11,18-20]. Four cases of subependymoma with H3K27M mutation did not possess glioma's molecular pathologic characteristics, for instance, *KIAA1549-BRAF* fusion, *BRAF* V600E mutation, *IDH1R132H*, *TP53* mutation, *ATRX* mutation, and 1p19q co-deletion. And no H3K27M mutations were found in any case of brain stem ependymoma whether in this cohort or in literature. Our study suggests that nuclear H3K27M expression may potentially be a sensitive and specific marker for brain stem subependymoma, which may be helpful in differentiating patients with ependymoma in brain stem.

It must be noted that our study is limited to a relatively small number of subependymomas and ependymomas (grade II and grade III). For this reason, our results are suggestive but not conclusive for clinical practice with respect to the higher sensitivity of H3K27M mutation in the differential diagnosis of brain stem subependymoma versus brain stem ependymoma.

Ethical approval

All procedures performed in studies involving human participants were in accordance with the ethical standards of the institutional.

This article does not contain any studies with animals performed by any of the authors.

Informed consent

Informed consent was obtained from all individual participants included in the study.

References

[1] Hou Z, Wu Z, Zhang J, et al. Clinical features and management of intracranial subependymomas in children. J Clin Neurosci 2013;20:84-8.
[2] Scheithauer BW. Symptomatic subependymoma. Report of 21 cases with review of the literature. J Neurosurg 1978;49:689-96.
[3] Louis DN, Ohgaki H, Wiestler OD, et al. World Health Organization histological classification of tumours of the central nervous system. France: International Agency for Research on Cancer; 2016; . p. 102-3.
[4] Rushing EJ, Cooper PB, Quezado M, et al. Subependymoma revisited: clinicopathological evaluation of 83 cases. J Neurooncol 2007;85:297-305.
[5] Kong LY, Wei J, Haider AS, et al. Therapeutic targets in subependymoma. J Neuroimmunol 2014;277:168-75.
[6] Cure LM, Hancock CR, Barrocas AM, Sternau LL, CH A. Interesting case of subependymoma of the spinal cord. Spine J 2014;14:e9-12.
[7] Bernal García LM, Cabezudo Artero JM, Marcelo Zamorano MB, Gilete Tejero I. Fluorescence-guided resection with 5-aminolevulinic acid of subependymomas of the fourth ventricle: report of 2 cases: technical case report. Neurosurgery 2015(Suppl. 2):E364-71.
[8] Bi ZY, Ren XH, Zhang JT, Jia W. Clinical, radiological, and pathological features in 43 cases of intracranial subependymoma. J Neurosurg 2015;122:49-60.
[9] Schwartzentruber J, Korshunov A, Liu X-Y, et al. Corrigendum: driver mutations in histone H3.3 and chromatin remodeling genes in paediatric glioblastoma. Nature 2012;484:130.

[10] Sturm D, Witt H, Hovestadt V, et al. Hotspot mutations in H3F3A and IDH1 define distinctepigenetic and biological subgroups of glioblastoma. Cancer Cell 2012;22:425-37.
[11] Venneti S, Garimella MT, Sullivan LM, et al. Evaluation of histone 3 lysine 27 trimethylation (H3K27me3) and enhancer of Zest 2 (EZH2) in pediatric glial and glioneuronal tumors shows decreased H3K27me3 in H3F3A K27M mutant glioblastomas. Brain Pathol 2013;23:558-64.
[12] Nguyen AT, Colin C, Nanni-Metellus I, et al. Evidence for BRAF V600E and H3F3A K27M double mutations in paediatric glial and glioneuronal tumors. Neuropathol Appl Neurobiol 2015;41:403-8.
[13] Orillac C, Thomas C, Dastagirzada Y, et al. Pilocytic astrocytoma and glioneuronal tumor with histone H3K27M mutation. Acta Neuropathol Commun 2016;4:84.
[14] Pages M, Beccaria K, Boddaert N, et al. Co-occurrence of histone H3K27M and BRAF V600E mutations in paediatric midline grade I ganglioglioma. Brain Pathol 2018;28:103-11.
[15] Huang TY, Piunti A, Lulla RR, et al. Detection of histone H3 mutations in cerebrospinal fluid-derived tumor DNA from children with diffuse midline glioma. Acta Neuropathol Commun 2017;5:28.
[16] Hochart A, Escande F, Rocourt N, et al. Long survival in a child with a mutated K27M-H3.3 pilocytic astrocytoma. Ann Clin Transl Neurol 2015;2:439-43.
[17] Gessi M, Capper D, Sahm F, et al. Evidence of H3K27M mutations in posterior fossa ependymomas. Acta Neuropathol (Berl) 2016;132(4):635-7.
[18] Bender S, Tang Y, Lindroth AM, et al. Reduced H3K27me3 and DNA hypomethylation are major drivers of gene expression in K27M mutant pediatric high-grade gliomas. Cancer Cell 2013;24:660-72.
[19] Chan KM, Fang D, Gan H, et al. The histone H3.3K27M mutation in pediatric glioma reprograms H3K27 methylation and gene expression. Genes Dev 2013;27:985-90.
[20] Lewis PW, Muller MM, Koletsky MS, et al. Inhibition of PRC2 activity by a gain-of-function H3 mutation found in pediatric glioblastoma. Science 2013;340:857-61.